Line shape of a transition between two levels in a three-level Λ configuration

Hyok Sang Han, Ji Eun Jeong, and D. Cho*
Department of Physics, Korea University, Seoul 136-713, Korea
(Received 6 May 2011; published 2 September 2011)

We report on our study of the line shape of a transition between two levels in a three-level Λ configuration. By using Poisson statistics under the assumption that the atom stays in a two-level steady state before it is optically pumped to the reservoir state, we arrive at a simple analytic expression for the line shape of a three-level atom. This expression reveals a new type of saturation in the time domain, which is conceptually different from that of power-broadening in a two-level atom. It can also be used as a basis for more complicated situations of Doppler-broadened gaseous samples or pump-and-probe spectroscopy. We tested the theory experimentally in an ideal situation of slow pulsed ^{85}Rb atoms and found excellent agreement. Application to measurements of a branching ratio or a Franck-Condon factor of a diatomic molecule is discussed.

DOI: 10.1103/PhysRevA.84.032502 PACS number(s): 32.70.Jz, 32.80.Xx, 37.20.+j

I. INTRODUCTION

The Lorentzian line shape of a transition between two levels is one of the best known formulas in atomic spectroscopy. While the resonance frequency of the transition reveals the internal structure of an atom, the line shape tells us various relaxation mechanisms and interaction dynamics between light and atoms. Spontaneous decay of the excited state is represented as a natural linewidth, and saturation of the transition is embodied as a power-broadening. When two-level atoms are in a gaseous phase, the Lorentzian shape is convoluted with the Maxwell-Boltzmann distribution leading to a Voigt profile.

However, a closed two-level system is an exceptional case and most atoms or molecules have more than one ground state, forming a three-level Λ system. See Fig. 1. An alkali-metal atom with two ground hyperfine levels or a diatomic molecule with rovibrational levels are common examples. In such a system, atoms in the ground state $|g\rangle$ are transferred to the reservoir state $|r\rangle$ by an optical pumping process and the line shape exhibits saturation and broadening, which are conceptually different from those of the two-level system. The effect of optical pumping on a line shape has been extensively studied in the context of saturated absorption spectroscopy to explain size and shape as well as the occasional inversion of observed spectra [1,2]. This effect was also invoked to explain the line shape in a double-resonance optical pumping [3] and a sub-Doppler linewidth in an indium saturated absorption spectroscopy [4]. All of these studies were, however, pump-and-probe spectroscopy using gaseous samples, where two-level saturation and the Doppler effect played dominant roles. Considering its ubiquitous presence, it is surprising that a simple expression for the line shape of a transition between two levels in a Λ configuration has never been derived. Such an expression for a stationary three-level atom would be a counterpart to the Lorentzian line shape for a two-level atom.

In this paper, we consider a stationary three-level Λ system interacting with a single probe beam. We consider a spectroscopic situation in which (i) the atomic sample is optically thin, (ii) the probe intensity is low so that the two-level transition is far below saturation, and (iii) the fluorescent photons are detected by a broadband detector without spectral discrimination. We will present a simple analytic expression for the line shape and its experimental confirmation using a slow atomic beam.

II. THEORY

We consider a three-level system shown in Fig. 1. Initially atoms are in the $|g\rangle$ state. During $0 \leqslant t \leqslant \tau$, a near-resonant laser beam with $E(t) = E_0 \cos \omega t$ is illuminated to drive a transition to the excited state $|e\rangle$. Once excited, the atom can decay to either the $|g\rangle$ or $|r\rangle$ state with respective probabilities p and $1 - p$. The total decay rate is Γ. We are interested in the integrated fluorescence as a function of the detuning $\Delta\omega = \omega - \omega_0$, where ω_0 is the resonance frequency of the g-e transition. Starting from the optical Bloch equations for the system, we can adiabatically eliminate the coherences and obtain the following rate equations for the populations n_e, n_g, and n_r:

$$\begin{aligned} \dot{n}_e &= W n_g - (W + \Gamma) n_e, \\ \dot{n}_g &= -W n_g + (W + p\Gamma) n_e, \\ \dot{n}_r &= (1 - p)\Gamma n_e. \end{aligned} \tag{1}$$

W is the g-e transition rate from Fermi's golden rule,

$$W = \frac{1}{2} \frac{s}{4\Delta\nu^2 + 1} \Gamma, \tag{2}$$

where $\Delta\nu = \Delta\omega/\Gamma$ and s is the saturation parameter for the two-level system, $s = 2\,|\langle e \,|\, d \,|\, g\rangle|^2 E_0^2/\hbar^2\Gamma^2$, with d being an electric dipole moment operator. The adiabatic elimination can be justified by noting that while the coherences change at the rate of Γ, the populations change at W with $W/\Gamma = s \ll 1$.

Unlike a two-level system, where the fluorescence line shape can be deduced from a steady-state solution, in the Λ system the atoms are eventually optically pumped to the reservoir state, and at the steady state there is no fluorescence. We are interested in the number of photons scattered while the atom interacts with the laser beam,

$$G_R(\Delta\nu, \tau) = \int_0^\tau n_e(\Delta\nu, t)\Gamma dt. \tag{3}$$

*cho@korea.ac.kr

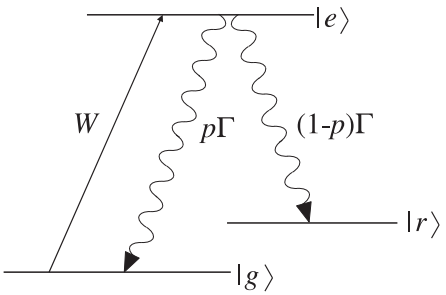

FIG. 1. A transition between two levels in a Λ configuration.

From the rate equations with the initial conditions, $n_g(0) = 1$ and $n_e(0) = n_r(0) = 0$, we obtain

$$G_R = \frac{W\Gamma}{2Q}\left[\frac{1-e^{-(W+\frac{\Gamma}{2}-Q)\tau}}{W+\Gamma/2-Q} - \frac{1-e^{-(W+\frac{\Gamma}{2}+Q)\tau}}{W+\Gamma/2+Q}\right], \quad (4)$$

where $Q = \sqrt{W^2 + pW\Gamma + \Gamma^2/4}$. Although the line shape is given in a closed form, it is rather complicated.

Alternatively, we calculate the number of emitted photons using Poisson statistics. We assume that while the atom stays within the (g, e) manifold, it is in a two-level steady state so that the photon scattering rate is

$$R(\Delta\nu) = \frac{1}{2}\frac{s}{4\Delta\nu^2 + 1 + s}\Gamma. \quad (5)$$

The probability for emitting n photons during $0 \leqslant t \leqslant \tau$ is

$$P(n) = \left[e^{-a}\frac{a^n}{n!}\right]p^n + \left[1 - e^{-a}\sum_{k=0}^{n-1}\frac{a^k}{k!}\right]p^{n-1}(1-p), \quad (6)$$

where $a = R\tau$. In the first term, the atom is in $|g\rangle$ after emitting n photons and in the second term it is in $|r\rangle$. Summation of the probabilities instead of the probability amplitudes is justified because each event of a spontaneous emission is an incoherent process. $P(n)$ satisfies the normalization condition, $\sum_{n=0}^{\infty} P(n) = 1$, and the expectation value of n, $G_P(\Delta\nu,\tau) = \sum_{n=1}^{\infty} nP(n)$, gives the fluorescence line shape in a compact form,

$$G_P(\Delta\nu,\tau) = \frac{1 - e^{-(1-p)R(\Delta\nu)\tau}}{1-p}. \quad (7)$$

In the limit of either $p \to 1$ or $R\tau \ll 1$, $G_P(\Delta\nu,\tau)$ reduces to the steady-state two-level case $R(\Delta\nu)\tau$, and when $\tau \gg \tau_e = 1/\Gamma$, it goes to $1/(1-p)$, which is the average number of photons scattered before the atom is optically pumped to the reservoir state. The above equation and Eq. (4) appear to be different. When τ is large enough, however, Eq. (4) reduces to Eq. (7). In fact, numerical evaluation with $p = 0.5$ shows that even when $s = 10$, the two line shapes are almost identical for $\tau \geqslant 200\tau_e$. The fractional discrepancy, $[G_P(\Delta\nu) - G_R(\Delta\nu)]/G_R(0)$, is less than 1.5×10^{-3} throughout the line shape.

Figure 2 shows numerically calculated line shapes using Eq. (7) when $p = 0.5$ and $s = 0.1$. When $\tau = 50\tau_e$, the line shape is basically Lorentzian. As τ increases to $200\tau_e$, however, the top becomes rounded, and eventually when $\tau = 1000\tau_e$, a plateau of height $1/(1-p)$ appears. When

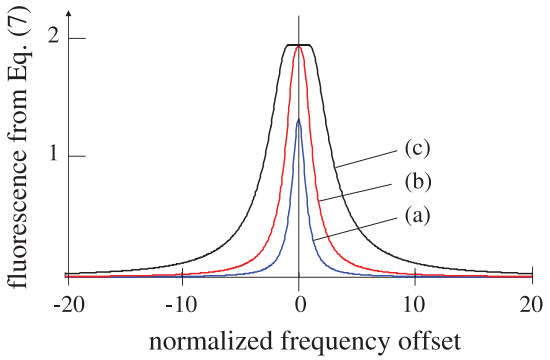

FIG. 2. (Color online) Calculated line shapes using Eq. (7) with $p = 0.5$. τ = (a) 50, (b) 200, and (c) $1000\tau_e$. Frequency offset from the resonance is normalized to Γ.

$\sigma = s(1-p)\tau/\tau_e$ is small, the full width at half-maximum (FWHM) in the unit of Γ is given approximately by $\sqrt{1+s+\sigma/2}$. When τ/τ_e is larger than 1, as s increases, the FWHM increases more rapidly than that of a two-level system, $\sqrt{1+s}$. When σ is large, the FWHM is approximately $\sqrt{\sigma/2\ln 2}$. We note that, for the three-level system, σ plays the role of a saturation parameter and that the saturation takes place in the time domain.

For an atomic beam from an effusive oven probed by a perpendicular laser beam, the expression in Eq. (7) can be used as a kernel for convolution with an atomic velocity distribution to find a fluorescence line shape:

$$F(\Delta\nu) = \frac{N}{1-p}\left[1 - 2\int_0^{\infty} x^3 e^{-x^2 - \frac{1}{x}(1-p)R\tau_0}dx\right]. \quad (8)$$

N is the number of atoms from the oven per unit time and τ_0 is the probe width w divided by $v = \sqrt{k_B T/m}$. T is the oven temperature and m is the atomic mass. If we consider a $D2$ transition of Rb [5] when $T = 200\,^{\circ}\mathrm{C}$, $s = 0.1$, and $p = 0.5$, $F(\Delta\nu)$ appears to be Lorentzian for small w. However, even for $w = 1$ mm, the FWHM is 1.6 times Γ. For w larger than 2.5 mm, the plateau becomes apparent. In spectroscopy using trapped [6,7] or slow atoms [8], the σ saturation is inevitable.

Although we considered the case of uniform probe field in Eq. (7), an atomic beam may experience time-varying probe intensity as it traverses, for example, a Gaussian beam. In this case, for an atom with a well-defined velocity v, the line shape can be written as

$$G(\Delta\nu) = \int_{-\infty}^{+\infty} e^{-(1-p)\overline{R(t)}t} R(t)dt, \quad (9)$$

where

$$\overline{R(t)} = \frac{1}{t}\int_{-\infty}^{t} R(t')dt',$$

and $R(t)$ is the photon scattering rate in Eq. (5) of the atom at t.

III. EXPERIMENT

In order to study the line shape and the saturation behavior experimentally, we use the $D1$ transition of ^{85}Rb from the $|g\rangle = |5S_{1/2}, F = 2\rangle$ to the $|e\rangle = |5P_{1/2}, F = 2\rangle$ state. The other ground hyperfine state $|r\rangle = |5S_{1/2}, F = 3\rangle$ plays

the role of the reservoir state. The branching ratio of the $|e\rangle \rightarrow |g\rangle$ decay is 2/9. The lifetime τ_e is 29.4 ns and Γ is $2\pi \times 5.41$ MHz. The $D1$ transition is preferred to the $D2$ because the hyperfine structure of the $5P_{1/2}$ state is simpler. We aim to separate the saturation behavior of the Λ configuration from the power broadening of the two-level system and use $s \approx 0.2$. We also use an atomic beam from a low-velocity intense source (LVIS) [8].

Our LVIS beam has a standard deviation of only 3 m/s around $\bar{v} = 11$ m/s [9] and it provides a few advantages: (i) The narrow velocity distribution allows direct comparison of the measured line shapes with Eq. (7) without the convolution in Eq. (8). (ii) The low velocity allows us to observe the saturation and the plateau with a narrow probe beam. At $w = 1$ mm, $\tau = 3100\,\tau_e$. Because we have to collect photons emitted by an atom anywhere in the probe beam with equal efficiency, it is advantageous to have a narrow beam. (iii) An LVIS can be operated in a pulsed mode and it increases the signal-to-noise ratio substantially. Even when saturated, an atom emits only $1/(1-p) = 9/7$ photons on average, and scattered background photons can easily swamp the signal. For the same number of sample atoms, we have to integrate the photodetector output over a much shorter period of time in the case of pulsed operation than in a continuous beam.

Figure 3 shows the beam machine. It consists of an LVIS built around a cube and a probe region. A gold-coated quarter-wave plate with a 2-mm diameter hole is placed on the downstream side of the cube. The atomic and the probe beams intersect at the center of another cubical chamber at 13 cm downstream from the LVIS center. In designing the probe chamber, special care was taken to maximize fluorescence detection and minimize the scattered photon background. A spherical mirror at the bottom reflects and a polished copper cylinder at the top guides the fluorescent photons to the 28-mm diameter detector at the top of the cube (inset in Fig. 3). Because we do not want to discriminate photons originating from the extended probe area, no imaging optics are employed. A pair of 20-cm-long tubes with Brewster windows on both sides of the cube guide the probe beam in and out of the interaction region. There are three annuli in each tube to block the photons scattered from the windows. Inside of the tubes and the annuli are coated with graphite to minimize stray reflections. With these precautions, only 1×10^{-5} of the probe power contributes to the background.

Two extended-cavity diode lasers (ECDL's) provide the trapping and repumping power for the LVIS magneto-optical trap (MOT). To produce the probe beam, a master ECDL is locked to the $|r\rangle = |5S_{1/2}, F = 3\rangle$ to $|e\rangle = |5P_{1/2}, F = 2\rangle$ transition and a slave ECDL is, in turn, locked to it with a frequency offset of around 3 GHz provided by a frequency synthesizer. The probe is scanned around the $|g\rangle = |5S_{1/2}, F = 2\rangle$ to $|e\rangle$ transition by scanning the synthesizer. The probe beam is transferred via a polarization-maintaining single-mode optical fiber. Its output is transformed to a vertically elongated shape with the e^{-2} intensity diameters of 6.4 and 2.8 mm. It goes through a linear polarizer and the output power is stabilized with an acousto-optic modulator placed upstream of the fiber. Then the beam width is defined by a variable slit and 1:1 imaged to the interaction region by a lens with a 17.5 cm focal length. In the measurement, the maximum slit width is 1 mm so that the probe beam intensity is uniform to within $\pm 10\%$. We assume that it is constant and use Eq. (7) instead of Eq. (9) in comparing the measured line shapes with the theory.

A measurement cycle begins with loading the LVIS for 2 s while the plug beam keeps atoms from being pushed toward the hole. The plug beam is blocked ($t = 0$) and a pulse of atoms is launched. Because the MOT beam along the beam machine, which pushes the atoms, does not contain a repumping component, atoms are optically pumped to the $|g\rangle = |5S_{1/2}, F = 2\rangle$ state on their way to the probe region. At $t = 10$ ms, the MOT beams are shuttered off and the anti-Helmholtz coil for the MOT is turned off. At $t = 14$ ms, atoms arrive at the probe region and begin to interact with the probe beam, which is always on. The fluorescence is integrated for 14 ms, and after a 36-ms delay the detector output is integrated again to measure the background. The frequency synthesizer is stepped up and the whole cycle is repeated. The scan is repeated a few times to obtain an average line shape.

IV. RESULTS AND DISCUSSION

We made two sets of measurements. In the first set, we study the low saturation regime with small σ. We fix the probe width w to 50 μm or $\tau = 155\tau_e$ and change the

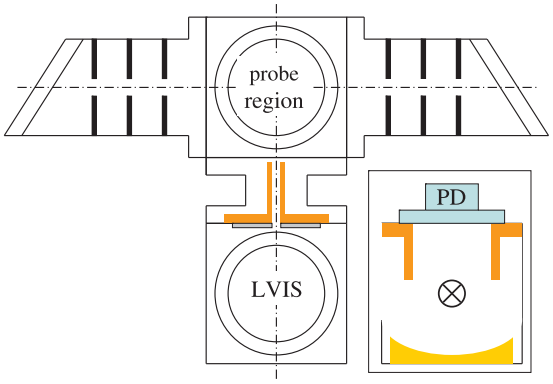

FIG. 3. (Color online) The beam machine consisting of a low-velocity intense source and a probe region. The inset shows the side view of the probe region. PD denotes photodiode.

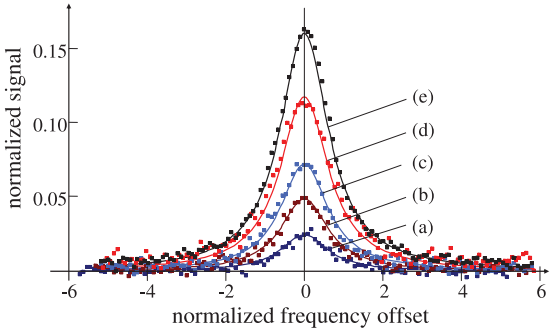

FIG. 4. (Color online) Line shapes at the low saturation regime. The probe beam width is 50 μm and the probe intensities are (a) 0.018, (b) 0.036, (c) 0.054, (d) 0.09, and (e) 0.13 mW/cm^2. The signals are normalized to that at the plateau, $I_P = 3.6$ mW/cm^2 and $w = 200$ μm. Solid lines are the theory curves from Eq. (10).

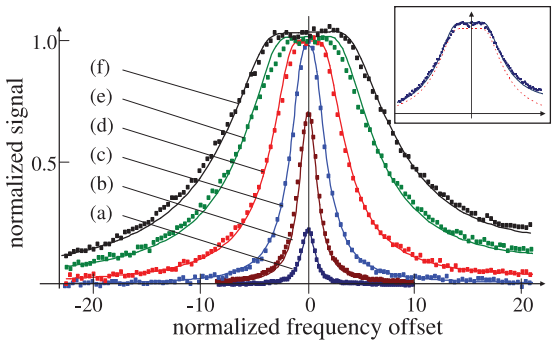

FIG. 5. (Color online) Line shapes toward the high saturation regime. The probe intensities are (a) 0.18, (b) 0.9, and (c) 3.6 mW/cm^2 at $w = 50$ μm. The probe beam widths are (d) 200, (e) 600, and (f) 1000 μm at $I_P = 3.6$ mW/cm^2. The inset shows the asymmetric line shape for $I_P = 5$ mW/cm^2 and $w = 1$ mm. Solid line is from Eq. (10) and the dotted line is without the second term in Eq. (10).

probe intensity I_P from 0.018 to 0.13 mW/cm^2. Because of diffraction and limited mechanical precision of the slit, it is not practical to reduce w below 50 μm. The results are shown in Fig. 4. In the second set, we aim to confirm the validity of Eq. (7) and demonstrate the time-domain saturation of the Λ configuration. We increase I_P from 0.18 to 3.6 mW/cm^2 at $w = 50$ μm and then increase w from 50 μm to 1 mm or $\tau = 3100\tau_e$ at $I_P = 3.6$ mW/cm^2. The results are shown in Fig. 5. Measured signals in both data sets are normalized to the value at the plateau of $I_P = 3.6$ mW/cm^2 and $w = 200$ μm.

In order to compare the observed line shapes in Figs. 4 and 5 with Eq. (7), we have to first find the saturation intensity I_S for the $|g\rangle = |5S_{1/2}, F = 2\rangle$ to $|e\rangle = |5P_{1/2}, F = 2\rangle$ transition. For unpolarized atoms, I_S is 17.7 mW/cm^2. However, atoms from the LVIS are produced by a circularly polarized light and their Zeeman distribution is not known. We use I_S as a fitting parameter and find that $I_S = 20$ mW/cm^2 gives the best fit to all the data. When $I_P = 3.6$ mW/cm^2, $s = 0.18$. In addition, even for the line shape (a) in Fig. 4 with $\sigma = 0.11$, the FWHM is 7.9 MHz. We think that the extra width is contributed by a residual Doppler shift from the transverse atomic motion, a Zeeman shift by ambient field, and laser frequency fluctuations. We incorporate this extra width by adding $\epsilon = 1.1$ to the denominator of R in Eq. (5): $R(\Delta\nu) = s\Gamma/2(4\Delta\nu^2 + 1 + \epsilon + s)$. Finally, we note that when $w \geqslant 200$ μm, the plateau keeps on rising and the line shape becomes asymmetric. See the inset in Fig. 5 for $I_P = 5$ mW/cm^2 and $w = 1$ mm. This is due to the $|g\rangle$ to $|e'\rangle = |5P_{1/2}, F = 3\rangle$ transition, which is 362 MHz blue detuned from the g-e transition. The saturation intensity for the g-e' transition is $I'_S = 5.1$ mW/cm^2 and the $|e'\rangle$ state decays to the $|g\rangle$ state with a probability $p' = 5/9$. When $I_P = 5$ mW/cm^2 and $w = 1$ mm, the FWHM of the parasitic transition is 168 MHz, and its effect on our main transition is apparent.

From these considerations, we use as a fitting function

$$g(\Delta\nu) = (1 - p)[G_P(\Delta\nu, \tau) + G'_P(\Delta\nu - \nu_0, \tau)], \quad (10)$$

where $R(\Delta\nu) = s\Gamma/2(4\Delta\nu^2 + 1 + \epsilon + s)$ and for the second term $\nu_0 = 67$, $p' = 5/9$, and $I'_S = 5.1$ mW/cm^2. Note that $g(\Delta\nu)$ is normalized to 1 when the contamination from the parasitic transition is neglected. The theoretical curves are represented as solid lines in Figs. 4 and 5 and they show excellent agreement with the data.

V. SUMMARY

In summary, we derived a simple analytic expression for the line shape of a transition between two levels in a Λ configuration. It is a three-level counterpart to the Lorentzian line shape of a two-level system. We compared the theory with the line shapes obtained in an ideal experimental situation. We note that one can measure a branching ratio in a Λ configuration or a Franck-Condon factor of a diatomic molecule by comparing the sizes of the plateaus. In the recent work on a CaF beam [10], the rate equations involving four levels were numerically integrated to extract the excited-state lifetime and Franck-Condon factor from the observed line shape.

ACKNOWLEDGMENTS

We thank M. R. Tarbutt for valuable discussions. This work was supported by the National Research Foundation of Korea (Grant No. 2009-0080091).

[1] M. S. Feld, M. M. Burns, T. U. Kühl, and P. G. Pappas, Opt. Lett. **5**, 79 (1980).
[2] P. R. Berman, P. F. Liao, and J. E. Bjorkholm, Phys. Rev. A **20**, 2389 (1979).
[3] H.-R. Noh and H. S. Moon, Phys. Rev. A **80**, 022509 (2009).
[4] J. I. Kim, D. Haubrich, B. Klöter, and D. Meschede, Phys. Rev. A **80**, 063801 (2009).
[5] L. R. Hunter, D. Krause Jr., K. E. Miller, D. J. Berkeland, and M. G. Boshier, Opt. Commun. **94**, 210 (1992).
[6] C. W. Oates, K. R. Vogel, and J. L. Hall, Phys. Rev. Lett. **76**, 2866 (1996).
[7] M. Maric, J. J. McFerran, and A. N. Luiten, Phys. Rev. A **77**, 032502 (2008).
[8] Z. T. Lu, K. L. Corwin, M. J. Renn, M. H. Anderson, E. A. Cornell, and C. E. Wieman, Phys. Rev. Lett. **77**, 3331 (1996).
[9] M. S. Jun, C. Y. Park, and D. Cho, J. Korean Phys. Soc. **33**, 260 (1998).
[10] T. E. Wall, J. F. Kanem, J. J. Hudson, B. E. Sauer, D. Cho, M. G. Boshier, E. A. Hinds, and M. R. Tarbutt, Phys. Rev. A **78**, 062509 (2008).